Critical dynamics of stochastic models with two conserved densities (model C′)

R. Folk[1] and G. Moser[2]
[1]*Institute for Theoretical Physics, University of Linz, Linz, Austria*
[2]*Institute for Physics and Biophysics, University of Salzburg, Salzburg, Austria*
(Received 22 October 2004; published 23 February 2005)

We calculate the field-theoretic functions of the generalized dynamical model $C^{*\prime}$, where two conserved secondary densities are coupled to a nonconserved complex order parameter (OP), in two-loop order. A transformation to "orthogonalized" densities can be performed where only one secondary density with nontrivial static coupling to the OP exists while the second one remains Gaussian. The secondary densities remain dynamically coupled by the nondiagonal diffusion coefficent. General relations for the field-theoretic functions allow us to relate the asymptotic critical properties of model $C^{*\prime}$ to the simpler model C^* with only one conserved density coupled to the OP. The nonasymptotic properties, however, differ as can be seen from the flow of the dynamic parameters, which is presented for the case of a real OP with componets $n=1,2,3$.

DOI: 10.1103/PhysRevE.71.026118 PACS number(s): 05.70.Jk, 64.60.Ak, 64.60.Ht

I. INTRODUCTION

The universal critical properties of dynamic critical behavior may be separated into different universality classes depending on the structure of the set of dynamical equations in addition to the separation into static universality classes [1]. The set of dynamical equations contains the slow densities—that is the order parameter density (OPD)—because of the critical slowing down and other densities of conserved quantities in the system [secondary densities (SD's)]. Moreover, it is important in which way these SD's couple to the OPD and with each other. One may have reversible couplings found from Poisson bracket relations [2], static couplings in the Hamiltonian, and/or a coupling via the irreversible part in the equations (diffusive terms in the equations of motion).

The structurally simplest model in this respect is model C, where the nonconserved OPD is coupled via a static term to one SD [3]. This model is highly nontrivial and its critical properties have been resolved only recently [4]. Another important aspect is that model C with OP dimension n is the limiting case of more complicated models with reversible terms. One example for $n=2$ is model F′ describing the critical dynamics of ^{3}He-^{4}He mixtures (see [5] for the model and [6] for a quantitative comparison of theory [7] with experiment). However, this model contains *two* conserved densities coupling to the OPD. Thus it seems to be worthwile to generalize model C to the case of more than one secondary density (model $C^{*\prime}$). Moreover, the properties are of interest when one wants to describe the tricritical behavior and/or the crossover between tricritical and the usual second-order transition behavior for ^{3}He-^{4}He mixtures. Nevertheless, model C′ might be of interest in itself. One might also think of applications to segragating systems (alloys) described by model C. The order parameter in these systems is nonconserved and couples to the concentration of one component [8,9]. If one adds the energy density, model C′ is obtained.

From model C one knows that there are three regions depending on the number of components of the OPD (see Fig. 1 and compare Fig. 1 in [10]): region I_a where the SD decouples from the OPD and model C reduces to model A [11]; region I_b (weak scaling) where the OPD and the SD scale differently, the OPD with the model A dynamic critical exponent $z=2+c\eta$ and the secondary density with $z=2+\alpha/\nu$ where α is the positive specific heat exponent and ν the correlation length exponent; region II (strong scaling) where all densities scale with $z=2+\alpha/\nu$. In the last region the fixed point value of the time scale ratio w^* of the relaxation rate of the OPD and diffusion constant of the SD is finite and nonzero, while in the other regions it is zero. This means that in regions I the OPD is much slower than the SD. The reverse situation of the SD being slower than the OPD ($w^*=\infty$) is not a stable fixed point [12].

As we can expect from other models containing additional conserved densities like model F′ and model E′ [13] the additional conserved density does not change the asymptotic

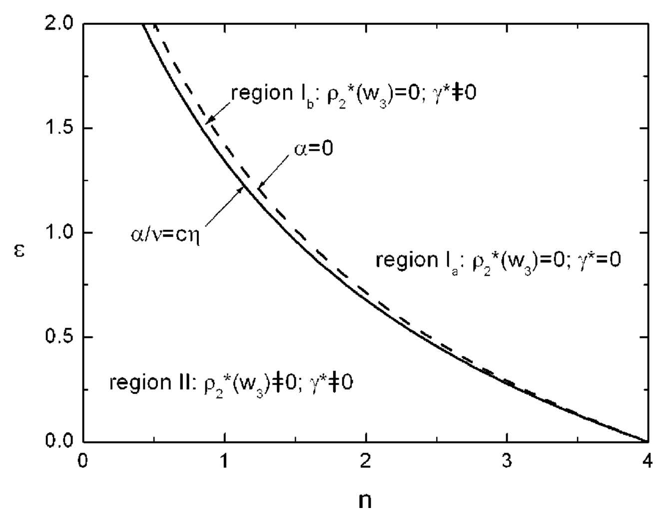

FIG. 1. Regions of different dynamical critical behavior in the ϵ-n plane ($\epsilon=4-d$), which are defined by the stable fixed point values of the static coupling γ and the dynamic parameter ρ_2. The fixed point value of the second dynamic parameter ρ_1 and the imaginary part of ρ_2 are always zero. The borderlines are defined by the conditions indicated.

critical properties of the OP. This was guaranteed by certain structural properties of the field theoretic functions valid independent of the perturbational order of the explicit field theoretic calculation. This is the case for model C$^{*\prime}$ too. General relations of the model- C$^{*\prime}$ field-theoretic functions prove that the asymptotic critical behavior of the OP is the same as in the simpler model C*. Restricting the analysis to the case of a real OP we show that although the fixed point values of the dynamic parameters depend on a new time scale ratio w_3, the dynamic critical exponents are the same as in model C (see Fig. 1).

The paper is organized as follows: After setting up the model equations (Sec. II), the model is renormalized in Sec. III and the relevant field-theoretic functions are calculated in two-loop order. Then it is shown that the asymptotic critical properties can be mapped onto model C (Sec. IV) and in Sec. V the nonasymptotic flow is considered. After the Conclusion some details of the calculations are contained in the Appendixes.

II. MODEL C$^{*\prime}$ EQUATIONS

We consider a system including a complex nonconserved OP $\vec{\psi}_0(x,t)$ and two real conserved secondary densities $m_{10}(x,t)$ and $m_{20}(x,t)$. The order parameter is assumed to be a vector with $n/2$ ($n=2,4,\ldots$) components [14]. The two secondary densities are scalar quantities. The critical dynamics of the nonconserved OP is purely relaxational while the dynamics of the conserved secondary densities is determined by a diffusive mode. This leads to the dynamic equations

$$\frac{\partial\vec{\psi}_0}{\partial t} = -2\mathring{\Gamma}\frac{\delta H}{\delta\vec{\psi}_0^+} + \vec{\theta}_\psi, \tag{1}$$

$$\frac{\partial\vec{\psi}_0^+}{\partial t} = -2\mathring{\Gamma}^+\frac{\delta H}{\delta\vec{\psi}_0} + \vec{\theta}_\psi^+, \tag{2}$$

$$\frac{\partial m_{10}}{\partial t} = \mathring{\lambda}\nabla^2\frac{\delta H}{\delta m_{10}} + \mathring{L}\nabla^2\frac{\delta H}{\delta m_{20}} + \theta_{m_1}, \tag{3}$$

$$\frac{\partial m_{20}}{\partial t} = \mathring{L}\nabla^2\frac{\delta H}{\delta m_{10}} + \mathring{\mu}\nabla^2\frac{\delta H}{\delta m_{20}} + \theta_{m_2}, \tag{4}$$

which we will call model C$^{*\prime}$ in the following. In the case of a real order parameter it reduces to model C$'$. The superscript + denotes complex-conjugated quantities. The kinetic coefficient of the OP $\mathring{\Gamma}=\mathring{\Gamma}'+i\mathring{\Gamma}''$ is assumed to be a complex quantity. The stochastic forces θ_{α_i} fulfill the relations

$$\langle\theta_{\psi_i}(x,t)\theta^+_{\psi_j}(x',t')\rangle = 4\mathring{\Gamma}'\delta(x-x')\delta(t-t')\delta_{ij}, \tag{5}$$

$$\langle\theta_{m_1}(x,t)\theta_{m_1}(x',t')\rangle = -2\mathring{\lambda}\nabla^2\delta(x-x')\delta(t-t'), \tag{6}$$

$$\langle\theta_{m_2}(x,t)\theta_{m_2}(x',t')\rangle = -2\mathring{\mu}\nabla^2\delta(x-x')\delta(t-t'), \tag{7}$$

$$\langle\theta_{m_1}(x,t)\theta_{m_2}(x',t')\rangle = -2\mathring{L}\nabla^2\delta(x-x')\delta(t-t'). \tag{8}$$

The critical behavior of the thermodynamic derivatives follows from the static functional

$$H\{\psi_0,m_{i0}\} = H_\psi\{\psi_0\} + H_m\{\psi_0,m_{i0}\}, \tag{9}$$

with an OP functional

$$H_\psi\{\psi_0\} = \int d^dx\left\{\frac{1}{2}\mathring{\tau}|\vec{\psi}_0|^2 + \frac{1}{2}\sum_{i=1}^{n/2}\sum_{\mu=1}^{d}\nabla_\mu\psi_{i0}\nabla_\mu\psi^+_{i0} + \frac{\mathring{\tilde{u}}}{4!}|\vec{\psi}_0|^4\right\} \tag{10}$$

and a secondary density functional

$$H_m\{\psi_0,m_{i0}\} = \int d^dx\left\{\frac{1}{2}m_{10}^2 + \frac{1}{2}m_{20}^2 + \frac{1}{2}\mathring{\gamma}m_{20}|\vec{\psi}_0|^2 - \mathring{h}m_{20}\right\}, \tag{11}$$

with $|\vec{\psi}_0|^2 \equiv \vec{\psi}_0^+\cdot\vec{\psi}_0$ [the center dot denotes a $(n/2)$-dimensional scalar product] and d is the spatial dimension. The static functional for the secondary densities (11) is of course not the general form for model C$^{*\prime}$. It contains already several special features. First, only one coupling $\mathring{\gamma}$ and one external field $\mathring{h}$, corresponding to the second secondary density m_{20}, are present while the first secondary density m_{10} appears in a Gaussian form. Second, the whole Gaussian part of the secondary densities is diagonal and static susceptibilities are absent. It is obtained by some suitable "orthogonalization" of the general form of the static functional, which usually appears. A subsequent scaling of the densities leads to the static functional in Eq. (11). Details concerning these transformations are described in Appendix A.

The above static functional may be reduced to the Ginzburg-Landau-Wilson functional with complex OP by integrating out the secondary density.

$$H_{GLW} = \int d^dx\left\{\frac{1}{2}\mathring{r}|\vec{\psi}_0|^2 + \frac{1}{2}\sum_{i=1}^{n/2}\sum_{\mu=1}^{d}\nabla_\mu\psi_{i0}\nabla_\mu\psi^+_{i0} + \frac{\mathring{u}}{4!}|\vec{\psi}_0|^4\right\}. \tag{12}$$

The parameters r and u in Eq. (12) are related to τ, $\tilde{u}$, γ, and h in Eq. (9) by

$$\mathring{r} = \mathring{\tau} + \mathring{\gamma}\mathring{h}, \quad \mathring{u} = \mathring{\tilde{u}} - 3\mathring{\gamma}^2. \tag{13}$$

The choice of a $(n/2)$-component OP in the equations above guarantees that the static functionals (9) and (12), and also all static properties derived from them, are fully equivalent to the corresponding static properties of a system with a real n-component order parameter (then with $n=1,2,\ldots$). The ability to eliminate the secondary density part (11) in Eq. (9) also leads to relations between the correlations of the secondary density m_{20} and the OP correlations. For the first and second cumulants one obtains

$$\langle m_{20}(x)\rangle = \mathring{h} - \mathring{\gamma}\left\langle\frac{1}{2}|\vec{\psi}_0(x)|^2\right\rangle, \tag{14}$$

$$\langle m_{20}(x)m_{20}(0)\rangle_c = 1 + \mathring{\gamma}^2\left\langle \frac{1}{2}|\vec{\psi}_0(x)|^2\frac{1}{2}|\vec{\psi}_0(0)|^2\right\rangle_c. \quad (15)$$

Note that the angular brackets in Eqs. (14) and (15) have to be calculated with a probability density $\exp(-H)/\mathcal{N}$ on the left-hand side and with $\exp(-H_{GLW})/\mathcal{N}'$ on the right-hand side, where $\mathcal{N}$ and $\mathcal{N}'$ are appropriate normalization factors. The external field $\mathring{h}$ is chosen to eliminate the finite expectation value of m_{20}. Choosing

$$\mathring{h} = \mathring{\gamma}\left\langle \frac{1}{2}|\vec{\psi}_0(x)|^2\right\rangle \quad (16)$$

from Eq. (14) immediately follows $\langle m_{20}(x)\rangle = 0$.

III. RENORMALIZATION OF MODEL C*′

Using the static functional (9) the renormalization of the static parameters is quite analogous to model C (for details see Appendix B in [10]). The secondary density m_{20} and all couplings and coefficients belonging to it correspond to the secondary density m_0 in [10]. The additional secondary density m_{10} does not couple to the order parameter. Therefore no perturbational contributions arise from this density and no new renormalization is needed compared to model C. This outlines the advantage in using the static functional with Eq. (11) instead of Eq. (A1).

In dynamics the kinetic coefficients Γ and Γ^+ renormalize identical to model C*: namely,

$$\mathring{\Gamma} = Z_\Gamma \Gamma, \quad \mathring{\Gamma}^+ = Z_\Gamma^+ \Gamma^+. \quad (17)$$

The kinetic coefficients of the secondary densities renormalize as

$$\mathring{\lambda} = Z_\lambda \lambda, \quad \mathring{L} = Z_L L, \quad \mathring{\mu} = Z_\mu \mu. \quad (18)$$

Note that the coefficient μ here corresponds to λ in [10]. In the present dynamic model mode couplings are absent. Therefore we simply have

$$Z_\lambda = 1, \quad Z_L = Z_{m_2}, \quad Z_\mu = Z_{m_2}^2, \quad (19)$$

where Z_{m_2} is the renormalization factor of m_2 (corresponding to Z_m in [10]).

A. ζ and β functions

We will use in statics and dynamics the same definition for each ζ function,

$$\zeta_{a_i}(\{\alpha_j\}) = \frac{d \ln Z_{a_i}^{-1}}{d \ln \kappa}, \quad (20)$$

in the following, where $\{\alpha_j\}=\{u,\gamma,\Gamma,\Gamma^+,\lambda,\mu,L\}$ is the set of static and dynamic model parameters. a_i represents any density ψ, m_{i0} or any model parameter α_i.

Because the secondary density m_{10} does not cause any additional renormalization in statics when Eq. (11) is used, all static ζ functions, and the relations between them, are identical to those presented in [10] for model C*/C. Also the ζ functions of the kinetic order parameter coefficients Γ, Γ^+ are defined and calculated analogously to [10] [compare Eqs. (16) and (17) therein]. The only difference is that they now depend also on the additional kinetic coefficients of the secondary densities. The corresponding ζ functions follow from Eqs. (19),

$$\zeta_\lambda(u,\gamma) = 0, \quad \zeta_L(u,\gamma) = \zeta_{m_2}(u,\gamma), \quad \zeta_\mu(u,\gamma) = 2\zeta_{m_2}(u,\gamma), \quad (21)$$

and are determined by the static ζ function

$$\zeta_{m_2}(u,\gamma) = \frac{1}{2}\gamma^2 B_{\psi^2}(u). \quad (22)$$

The function $B_{\psi^2}(u)$ is connected to renormalization of the specific heat and has been defined in [10].

Introducing time scale ratios

$$w_1 = \frac{\Gamma}{\lambda}, \quad w_2 = \frac{\Gamma}{\mu}, \quad w_3 = \frac{L}{\sqrt{\lambda\mu}}, \quad (23)$$

we immediately obtain the corresponding ζ functions as

$$\zeta_{w_1}(u,\gamma,\{w\}) = \zeta_\Gamma(u,\gamma,\{w\}), \quad (24)$$

$$\zeta_{w_2}(u,\gamma,\{w\}) = \zeta_\Gamma(u,\gamma,\{w\}) - \gamma^2 B_{\psi^2}(u), \quad (25)$$

$$\zeta_{w_3}(u,\gamma,\{w\}) = 0. \quad (26)$$

The β functions for static or dynamic model parameters α_i are generally defined as

$$\beta_{\alpha_i}(\{\alpha_j\}) = \alpha_i(-c_i + \zeta_{\alpha_i}(\{\alpha_j\})), \quad (27)$$

where c_i is the naive cutoff dimension of the corresponding parameter obtained by power counting. The static β functions and flow equations are explicitly listed in [10]. The β functions of the time scale ratios w_i can be written as

$$\beta_{w_i}(u,\gamma,\{w\}) = w_i \zeta_{w_i}(u,\gamma,\{w\}), \quad (28)$$

with $i=1,2,3$, which follow immediately from Eq. (27). Since the cutoff dimension c_i of all kinetic coefficients is zero, it is zero also for all ratios w_i; see Eq. (23). The ζ functions are taken from Eqs. (24)–(26). The flow equations of the time scale ratios are given by

$$l\frac{dw_i}{dl} = \beta_{w_i}(u,\gamma,\{w\}). \quad (29)$$

Equation (26) implies that w_3 stays constant at its initial value and therefore appears like a fixed external parameter within the model [15]. The only dynamic ζ function ζ_Γ, which defines the dynamical critical exponent of the OP, has to be determined from dynamic perturbation expansion within model C*′. All other functions are known from the Ginzburg-Landau-Wilson model (12).

From the general structure of the β functions (28) we obtain immediately the flow equation for the ratio w_1/w_2 as

$$l\frac{d}{dl}\frac{w_1}{w_2} = \gamma^2 B_{\psi^2}(u), \tag{30}$$

which is completely determined by static quantities.

The above equations are valid in the complex model $C^{*\prime}$ as well as in the real model C'. In the first case $\{w\}$ is a place holder for $w_1, w_1^+, w_2, w_2^+, w_3$ (w_1 and w_2 are complex quantities); in the second case $\{w\}$ stands for w_1, w_2, w_3.

In the complex case the imaginary parts of w_1 and w_2 in Eqs. (23) are both related to the same imaginary part Γ'' of the kinetic coefficient of the order parameter (λ and μ are real quantities anyway). Thus w_1'' and w_2'' cannot be independent from each other. This means that the ratio w_1/w_2 has to be real even for complex w_i, which is verified in Eq. (30). From the condition $\mathrm{Im}(w_1/w_2)=0$ we obtain immediately

$$w_1'' = w_2''\frac{w_1'}{w_2'}. \tag{31}$$

B. Two-loop results

Using the model with the transformed static functional (11), the explicit two-loop expressions of the static ζ functions are identical to those of model C^*/C in [10] and can be taken from there. In order to simplify the dynamic perturbation expansion the dynamic ζ function ζ_Γ has been calculated within the dynamically diagonalized model (B8) and (B9) given in Appendix B leading to the expression (B14).

For the following considerations it is convenient to introduce

$$\rho_i = \frac{w_i}{1+w_i}, \quad i=1,2, \tag{32}$$

mapping the time scale ratios w_1 and w_2 onto a finite region of the complex plane. In the case of model C'' where w_1 and w_2 are real the corresponding parameters ρ_1 and ρ_2 fall into the interval $0 \leqslant \rho_i \leqslant 1$. Transforming the ζ_Γ function (B18) of the dynamically diagonal system back to the parameters of the dynamically nondiagonal model (23) and (32), respectively, we obtain

$$\begin{aligned}\zeta_\Gamma(u,\gamma,\rho_1,\rho_2,w_3) = {}& \zeta_\Gamma^{(A)}(u) + \frac{\rho_2\gamma^2}{1-W_3^2}\Bigg\{1 - \frac{n+2}{6}u(1-L_A) \\ &+ \frac{1}{2}\frac{\rho_2\gamma^2}{1-W_3^2}\left[\frac{n+2}{2}L_A - \frac{n}{2} + \frac{\rho_2+\rho_1 W_3^2}{1-W_3^2}\right]\Bigg\} \\ &- \frac{1}{2}\left(\frac{\gamma^2}{K_\rho}\right)^2(D_+ + D_-) \\ &- \frac{1}{2}\frac{w_3^2}{1-w_3^2}\left(\frac{\rho_1\rho_2\gamma^2}{K_\rho}\right)^2(D_\times^{(1)} + D_\times^{(2)}),\end{aligned} \tag{33}$$

with coefficients

$$W_3^2 = (1-\rho_1)(1-\rho_2)w_3^2 \tag{34}$$

and

$$K_\rho = \sqrt{(\rho_2-\rho_1)^2 + 4\rho_1\rho_2(1-\rho_1)(1-\rho_2)w_3^2}. \tag{35}$$

The parameters $D_\pm$ are defined as

$$D_\pm = \left(\frac{\pm(\rho_1-\rho_2)+K_\rho}{2}R_\pm\right)^2(1+R_\pm)\ln(1-R_\pm^2), \tag{36}$$

where we have introduced

$$R_\pm = \frac{2\rho_1\rho_2}{\rho_1+\rho_2\pm K_\rho}. \tag{37}$$

The cross coefficients $D_\times^{(i)}$ are

$$\begin{aligned}D_\times^{(1)} = {}& \left(2 - \frac{(\rho_1+\rho_2)\left(1+\dfrac{\rho_1\rho_2}{1-W_3^2}\right) - 4\rho_1\rho_2}{(1-\rho_1)(1-\rho_2)(1-w_3^2)}\right) \\ &\times \frac{1-\rho_1\rho_2-W_3^2}{1-W_3^2}\ln\left(1-\frac{\rho_1\rho_2}{1-W_3^2}\right),\end{aligned} \tag{38}$$

$$\begin{aligned}D_\times^{(2)} = {}& \frac{\rho_1^2\rho_2^2 K_\rho}{(1-\rho_1)(1-\rho_2)(1-w_3^2)(1-W_3^2)^2} \\ &\times\Bigg[\left(\frac{1}{R_+}-1\right)^2\ln\left(\frac{\rho_1+\rho_2-2\rho_1\rho_2}{R_-(1-W_3^2)}\right) \\ &- \left(\frac{1}{R_-}-1\right)^2\ln\left(\frac{\rho_1+\rho_2-2\rho_1\rho_2}{R_+(1-W_3^2)}\right)\Bigg].\end{aligned} \tag{39}$$

The contribution $\zeta_\Gamma^{(A)}(u)$ in Eq. (33) denotes the dynamic ζ function of model A. Its two-loop expression is given in Eq. (B16) in Appendix B. The above ζ function (33) is valid in both the complex and real models. The difference between the two cases lies in the expression for L_A. In the complex model $C^{*\prime}$ it reads

$$L_A = 2\ln\frac{2}{1+\dfrac{\Gamma^+}{\Gamma}} + \left(2+\frac{\Gamma}{\Gamma^+}\right)\ln\frac{\left(1+\dfrac{\Gamma^+}{\Gamma}\right)^2}{1+2\dfrac{\Gamma^+}{\Gamma}}, \tag{40}$$

with Γ, and w_1, w_2 respectively, as complex parameters, while in the real model C' (in the limit $\Gamma'' \to 0$) the function L_A reduces to the simple number

$$L_A = 3\ln\frac{4}{3}, \tag{41}$$

with w_1, w_2 also as real parameters (w_3 is always real).

The ζ function (33) reaches different interesting limits for special choices of its arguments.

1. Model $C^{*\prime}$ for $w_3 \equiv 0$

The first limit of interest is the case where the dynamic coupling L of the two secondary densities vanishes. The secondary density with index 1 has no static coupling to the order parameter. It couples only via the dynamic cross coefficient L, or w_3 respectively; see Eqs. (3) and (4). Thus setting $w_3=0$ the function has to reduce to the ζ function of model C^*/C from [10]. Taking into account

$$W_3 \overset{w_3=0}{\longrightarrow} 0, \quad K_\rho \overset{w_3=0}{\longrightarrow} \rho_2 - \rho_1, \tag{42}$$

following immediately from (34) and (35), the ζ function (33) indeed reduces to

$$\begin{aligned}\zeta_\Gamma(u,\gamma,\rho_1,\rho_2,0) &= \zeta_\Gamma^{(A)}(u) + \rho_2\gamma^2\Bigg\{1 - \frac{n+2}{6}u(1-L_A) \\ &\quad + \frac{1}{2}\rho_2\gamma^2\left[\frac{n+2}{2}L_A - \frac{n}{2} + \rho_2 - (1+\rho_2)\ln(1-\rho_2^2)\right]\Bigg\} \\ &= \zeta_\Gamma^{(C)}(u,\gamma,\rho_2),\end{aligned} \tag{43}$$

which corresponds to the model C*/C ζ_Γ function where the secondary density is indexed with 2 [compare Eq. (50) in [10]]. The contributions of the other secondary density completely drop out.

2. Model C$^{*\prime}$ for $\rho_1=0$

This is another limit of interest and it is equivalent to $w_1=0$ which means that the first secondary density is getting very fast compared to the order parameter. In this case it should not influence the critical behavior and the critical dynamics should also be determined by model C*/C. Equations (34) and (35) reduce to

$$W_3 \overset{w_1=0}{\longrightarrow} (1-\rho_2)w_3^2, \quad K_\rho \overset{w_1=0}{\longrightarrow} \rho_2. \tag{44}$$

Performing this limit one has to take into account that R_- becomes 0/0 (R_+ is simply 0). A careful examination reveals that we have

$$\lim_{\rho_1\to 0} R_- = \frac{\rho_2}{1-(1-\rho_2)w_3^2}, \tag{45}$$

leading to

$$\begin{aligned}\zeta_\Gamma(u,\gamma,0,\rho_2,w_3) &= \zeta_\Gamma^{(A)}(u) + \rho(\rho_2,w_3)\gamma^2\Bigg\{1 - \frac{n+2}{6}u(1-L_A) \\ &\quad + \frac{1}{2}\rho(\rho_2,w_3)\gamma^2\Bigg[\frac{n+2}{2}L_A - \frac{n}{2} + \rho(\rho_2,w_3) \\ &\quad - [1+\rho(\rho_2,w_3)]\ln[1-\rho^2(\rho_2,w_3)]\Bigg]\Bigg\} \\ &= \zeta_\Gamma^{(C)}(u,\gamma,\rho),\end{aligned} \tag{46}$$

with $\rho(\rho_2,w_3)$ as

$$\rho(\rho_2,w_3) = \frac{\rho_2}{1-(1-\rho_2)w_3^2}. \tag{47}$$

From Eq. (46) we can see that ρ_2 and w_3 only enter in the special combination (47). We obtain a model C*/C ζ function with a dynamic parameter ρ and therefore the whole critical dynamics is determined by model C*/C. All solutions concerning fixed points and stability of ρ can be taken from [10]. ρ_2 is then obtained by inverting Eq. (47) , which leads to

$$\rho_2 = \rho\frac{1-w_3^2}{1-\rho w_3^2}, \tag{48}$$

as a function of the model C*/C parameter ρ and the external parameter w_3.

3. Model C$^{*\prime}$ for $\rho_2=0$

This limit describes a model where the secondary density, which couples with γ to the OP, is getting very fast and therefore unimportant in the critical region. From Eq. (33) we obtain

$$\zeta_\Gamma(u,\gamma,\rho_1,0,w_3) = \zeta_\Gamma^{(A)}(u). \tag{49}$$

In this case the critical dynamics is completely described by model A.

IV. ASYMPTOTIC PROPERTIES OF MODEL C$^{*\prime}$/C$'$

The asymptotics of the model is essentially determined by the fixed points and their stability from which the critical exponents follow. From Eq. (9) it follows that the static fixed points and their stability regions are the same as in model C*/C [10] where an extensive discussion has been performed.

A. Fixed points

Restricting the discussion to the stable fixed points we have to consider the Heisenberg fixed point $u^\star=u_H$ which is always stable ($d<d_c=4$) for all OP component numbers n. The stable fixed point for γ then depends on n. For Ising models with $n=1$ a finite fixed point $\gamma^\star=\gamma_C$ is stable, while in planar ($n=2$) and Heisenberg ($n=3$) models $\gamma^\star=0$ is the stable fixed point (this holds for all $n\geqslant 2$). u_H and γ_C have been calculated in several renormalization schemes. Within the minimal subtraction scheme the ϵ-expanded results in two-loop order can be taken from Eqs. (42) and (45) in [10], for instance. When Borel resummation is used the fixed point values for $u_H/24$ can be found in Table 2 of [16] for integer numbers $n=0,1,2,3$.

The dynamic fixed points $w_i^\star$ are determined by the zeros of the β functions (28) together with Eq. (24) and (25). But it is more approprate to consider the fixed points of the parameters ρ_i introduced in Eq. (47). From the definition (47) of ρ_i and the ζ functions (24) and (25) we obtain immediately

$$\beta_{\rho_1}(u,\gamma,\rho_1,\rho_2,w_3) = \rho_1(1-\rho_1)\zeta_\Gamma(u,\gamma,\rho_1,\rho_2,w_3), \tag{50}$$

$$\begin{aligned}\beta_{\rho_2}(u,\gamma,\rho_1,\rho_2,w_3) &= \rho_2(1-\rho_2)[\zeta_\Gamma(u,\gamma,\rho_1,\rho_2,w_3) \\ &\quad - \gamma^2 B_{\psi^2}(u)].\end{aligned} \tag{51}$$

Inserting a static fixed point $u^\star$, $\gamma^\star$ into Eqs. (50) and (51) we have to look for solutions $\rho_1^\star$ and $\rho_2^\star$ of the equations

$$\beta_{\rho_i}(u^\star,\gamma^\star,\rho_1^\star,\rho_2^\star,w_3) = 0, \quad i=1,2. \tag{52}$$

The above equations have always the four trivial solutions $(\rho_1^\star,\rho_2^\star)=(0,0),(0,1),(1,0),(1,1)$. The nontrivial fixed points with finite $\rho_1^\star$ or $\rho_2^\star$ are determined by the equations

$$\zeta_\Gamma(u^\star,\gamma^\star,\rho_1^\star,\rho_2^\star,w_3)=0, \tag{53}$$

$$\zeta_\Gamma(u^\star,\gamma^\star,\rho_1^\star,\rho_2^\star,w_3)-\gamma^{\star 2}B_{\psi^2}(u^\star)=0. \tag{54}$$

The stable static fixed point $\gamma^\star$ determines which solutions of the above two equations are possible.

(i) In the cases $n\geqslant 2$, with $\gamma^\star=0$, we have [see Eq. (33)]

$$\zeta_\Gamma(u_H,0,\rho_1^\star,\rho_2^\star,w_3)=\zeta_\Gamma^{(A)}(u_H)\neq 0. \tag{55}$$

The two equations (53) and (54) reduce to the same equation without any solution. Thus in this case no fixed point values $\rho_i^\star$ different from 0 or 1 are possible.

(ii) In the case $n=1$, with $\gamma^\star=\gamma_C$, we obtain, from Eqs. (53) and (54),

$$\zeta_\Gamma(u_H,\gamma_C,\rho_1^\star,\rho_2^\star,w_3)=0, \tag{56}$$

$$\zeta_\Gamma(u_H,\gamma_C,\rho_1^\star,\rho_2^\star,w_3)-\gamma_C^2B_{\psi^2}(u_H)=0. \tag{57}$$

Assuming that we have found a solution with $\rho_i^\star\neq 0$ which fulfills Eq. (56), the second equation would be in contradiction to the first since $\gamma_C^2B_{\psi^2}(u_H)\neq 0$. Thus a solution with both parameters $\rho_1^\star\neq 0$ and $\rho_2^\star\neq 0$ is not possible. The only nontrivial solution is $\rho_1^\star=0$, then Eq. (56) is obsolete according to Eq. (50) , and one has to solve

$$\begin{aligned}\zeta_\Gamma(u_H,\gamma_C,0,\rho_2^\star,w_3)-\gamma_C^2B_{\psi^2}(u_H)\\ =\zeta_\Gamma^{(C)}(u_H,\gamma_C,\rho^\star)-\gamma_C^2B_{\psi^2}(u_H)\\ =0\end{aligned} \tag{58}$$

for ρ_2 or ρ, where the first equality follows from Eq. (46). However, nothing has to be calculated since $\rho^\star=\rho^\star(\rho_2^\star,w_3)$ defined by Eq. (47) is given by the fixed point value determined already in model C*/C. Thus the fixed point $\rho_2^\star$ depends on the parameter w_3,

$$\rho_2^\star=\rho^\star\frac{1-w_3^2}{1-\rho^\star w_3^2}, \tag{59}$$

quite analogously to Eq. (48). In [10] we have shown that the complex model C* has the same fixed points as the real model C which was expressed by $\rho''^\star=0$, leading to a real nontrivial fixed point $\rho^\star=\rho'^\star$. From Eq. (59) follows immediately that $\rho_2^\star$ is also always real and that the complex model C$'^*$ and the real model C$'$ have the same fixed points. In Fig. 2 we have plotted the fixed point value of ρ_2 in the parameter interval $0\leqslant w_3\leqslant 1$ at the OP component number $n=1$ where Eq. (59) is the stable fixed point (see Table I and the next subsection). At $w_3=0$ the fixed point value $\rho_2^\star$ is equal to the model C*/C fixed point value $\rho^\star=0.33$.

Note that a solution $\rho_2^\star=0$ and $\rho_1^\star\neq 0$ is not possible. Due to Eq. (49) one would end up with the condition $\zeta_\Gamma^{(A)}(u_H)\overset{!}{=}0$ following from Eq. (56) , which is not true. A survey of all fixed points concerning the static Heisenberg fixed point u_H is given in Table I.

B. Stability

In order to obtain the dynamic transient exponents we have to consider the eigenvalues of the matrix

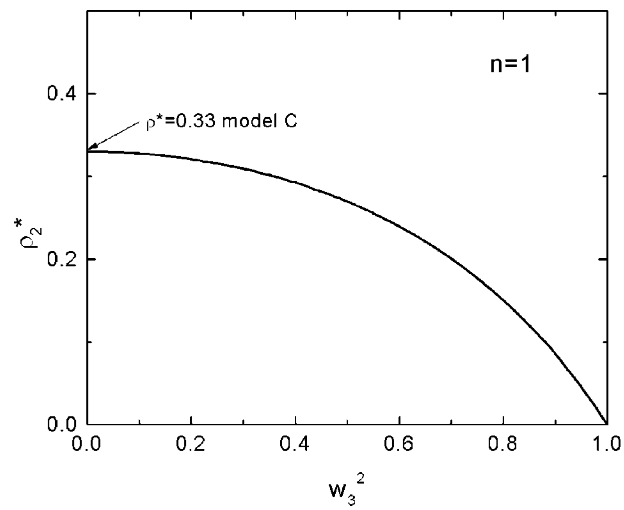

FIG. 2. Fixed point value for ρ_2 as function of the parameter w_3 at OP component number $n=1$ calculated from Eq. (59) .

$$\left[\frac{\partial\beta_{\rho_j}}{\partial\rho_i}\right]=\begin{pmatrix}\dfrac{\partial\beta_{\rho_1}}{\partial\rho_1} & \dfrac{\partial\beta_{\rho_2}}{\partial\rho_1}\\ \dfrac{\partial\beta_{\rho_1}}{\partial\rho_2} & \dfrac{\partial\beta_{\rho_2}}{\partial\rho_2}\end{pmatrix}. \tag{60}$$

Inserting the general structure (50) and (51) of the β functions into Eq. (60) we obtain the eigenvalues

$$\lambda_\pm=\frac{1}{2}[s_++G_1+G_2\pm\sqrt{(s_-+G_1+G_2)^2-4s_-G_2}], \tag{61}$$

with the definitions

$$s_\pm=(1-2\rho_1)\zeta_\Gamma\pm(1-2\rho_2)(\zeta_\Gamma-\gamma^2B_{\psi^2}) \tag{62}$$

and

$$G_i=\rho_i(1-\rho_i)\frac{\partial\zeta_\Gamma}{\partial\rho_i},\quad i=1,2. \tag{63}$$

The transient exponent ω is obtained by inserting a special fixed point into the eigenvalue (61). Thus we have

TABLE I. Overview of the fixed point values of model C$'^*$/C$'$ for the Heisenberg fixed point $u^\star=u_H$.

$\gamma^\star$	$\rho_1^\star$	$\rho_2^\star$	Stable for
0	0	0	$n=2,3,\ldots$
	0	1	-
	1	0	-
	1	1	-
γ_C	0	0	-
	0	1	-
	1	0	-
	1	1	-
	0	$\rho^\star(1-w_3^2)/(1-\rho^\star w_3^2)$	$n=1$

$$\omega_\pm(w_3) = \lambda_\pm(w_3)|_{\{\alpha\}=\{\alpha^*\}}, \tag{64}$$

where $\{\alpha\}$ represents the parameter set $\{u,\gamma,\rho_1,\rho_2\}$. For a stable fixed point all two transient exponents have to be positive. The parameter w_3 appears as an argument because it enters the expressions like an external parameter.

For the trivial fixed points $\rho_i=0,1$ we always have $G_i=0$ from Eq. (63). In these cases the transient exponents reduce to

$$\omega_+ = (1-2\rho_1^\star)\zeta_\Gamma(u_H,\gamma^\star,\rho_1^\star,\rho_2^\star,w_3), \tag{65}$$

$$\omega_- = (1-2\rho_2^\star)[\zeta_\Gamma(u_H,\gamma^\star,\rho_1^\star,\rho_2^\star,w_3) - \gamma^{\star 2}B_{\psi^2}(u_H)]. \tag{66}$$

Inserting the four combinations $(\rho_1^\star,\rho_2^\star)=(0,0),(0,1),(1,0),(1,1)$ into Eqs. (65) and (66) one can see that in the cases $(0,1)$, $(1,0)$, and $(1,1)$ at least one exponent is always negative independent of the value of $\gamma^\star$. These fixed points are unstable for all OP component numbers n. For $(\rho_1^\star,\rho_2^\star)=(0,0)$ we obtain, for $\gamma^\star=0$,

$$\omega_+ = \omega_- = \zeta_\Gamma^{(A)}(u_H) = c\eta > 0 \tag{67}$$

and, for $\gamma^\star=\gamma_C$,

$$\omega_+ = \zeta_\Gamma^{(A)}(u_H) = c\eta > 0, \tag{68}$$

$$\omega_- = \zeta_\Gamma^{(A)}(u_H) - \gamma_C^2 B_{\psi^2}(u_H) = c\eta - \frac{\alpha}{\nu}. \tag{69}$$

For planar $(n=2)$ and Heisenberg $(n=3)$ systems the static fixed point $\gamma^\star=0$ is stable. From Eq. (67) follows that $\rho_1^\star=\rho_2^\star=0$ is the stable dynamic fixed point in this case. In Ising $(n=1)$ systems $\gamma^\star=\gamma_C$ is stable and the dynamic transient exponents (68) and (66) are relevant. In this case ω_- is negative because $\alpha/\nu > c\eta$. Thus $\rho_1^\star=\rho_2^\star=0$ is unstable. We want to emphasize that at noninteger values of n a region in the n-d plane exists in which ω_- is positive and therefore the fixed point $\gamma^\star=\gamma_C$, $\rho_1^\star=0$ and $\rho_2^\star=0$ stable. The region is determined by the conditions $\alpha/\nu=0$ (border for the stable static fixed point $\gamma^\star=0$) and $\alpha/\nu=c\eta$ [border for ω_- in Eq. (69) to change sign] and is identical to the one in model C^*/C (see Fig. 1 here and in [10]).

Considering the nontrivial fixed point $\rho_1^\star=0$, $\rho_2^\star\neq 0$, the expressions in Eq. (63) reduce to $G_1=0$ and $G_2=\rho_2(1-\rho_2)(\partial\zeta_\Gamma/\partial\rho_2)$. The fixed point value $\rho_2^\star$ fulfills

$$\zeta_\Gamma(u_H,\gamma_C,0,\rho_2^\star,w_3) - \gamma_C^2 B_{\psi^2}(u_H) = 0. \tag{70}$$

Equation (62) reduces therefore to $s_+=s_-=\zeta_\Gamma(u_H,\gamma_C,0,\rho_2^\star,w_3)$ and the transient exponents turn into

TABLE II. Overview of the transient exponents of model C'^*/C' for the stable fixed points at several n. The exponents with superscript (b) are calculated with the Borel summed static functions, while for the one with superscript (l) ϵ-expanded statics has been used [17].

n	$\omega_+^{(b)}$	$\omega_-^{(b)}$	$\omega_+^{(l)}$	$\omega_-^{(l)}$
1	0.1766	0.0103	0.0988	0.0544
2	0.0304	0.0304	0.0145	0.0145
3	0.0312	0.0312	0.0150	0.0150

$$\omega_+ = \zeta_\Gamma(u_H,\gamma_C,0,\rho_2^\star,w_3), \tag{71}$$

$$\omega_- = \rho_2^\star(1-\rho_2^\star)\frac{\partial\zeta_\Gamma}{\partial\rho_2}_{\{\alpha\}=\{\alpha^\star\}}. \tag{72}$$

Using Eq. (70) we obtain immediately

$$\omega_+ = \gamma_C^2 B_{\psi^2}(u_H) = \frac{\alpha}{\nu}, \tag{73}$$

which is positive for Ising $(n=1)$ systems. With Eqs. (59) and (46) the transient exponent ω_- can be expressed by the known dynamic transient exponent $\omega_\rho^{(C)}$ of model C^*/C, which is plotted in Fig. 3 in [10]. It turns out that

$$\omega_- = \omega_\rho^{(C)}. \tag{74}$$

Thus we have proven that the stability regions and also the dynamic exponent z, respectively, are identical to model C^*/C in the whole n-d plane. The cross time scale ratio w_3 which couples the two secondary densities dynamically has no influence on the critical dynamical behavior. However, the fixed point values of ρ_2 and the nonasymptotic dynamic flow of the time scale ratios depend on the values of w_3.

From Table II one sees that the transient exponents are considerably small for all OP component numbers n considered. This leads to nonasymptotic behavior even very close to the critical point.

In Table III we summarize the dynamical critical exponents of the OP and the secondary densities in the different regions in the ϵ-n plane. The dynamic critical exponents are defined by the corresponding values of the Onsager coefficient ζ functions at the stable fixed point: i.e.,

$$z = 2 + \zeta_\Gamma^\star, \quad z_1 = 2, \quad z_2 = 2 + \zeta_\mu^\star. \tag{75}$$

In region I_a the secondary densities decouple at the fixed point $(\gamma^\star=0)$ and the time scale ratios $w_i^\star$ are both zero. The model reduces to model A with the corresponding dynamic

TABLE III. Overview of the dynamical critical and transient exponents of model C' in the different regions of the n-d plane (see Fig. 1). $\omega_\rho^{(C)}$ is the transient of model C.

Region	z	z_2	z_1	ω_+	ω_-
II	$2+\alpha/\nu$	$2+\alpha/\nu$	2	α/ν	$\omega_\rho^{(C)}$
I_b	$2+c\eta$	$2+\alpha/\nu$	2	$c\eta$	$c\eta-\alpha/\nu$
I_a	$2+c\eta$	2	2	$c\eta$	$c\eta$

exponent for the OP. The secondary densities have simply $z=2$ according to their conservation property. In region I_b one secondary density (indexed by 2) couples to the OP ($\gamma^\star \neq 0$) but the time ratios $w_i^\star$ stay zero. This is the region of weak scaling since due to the coupling to the OP the secondary density indexed by two scales nontrivially with $z_2=2+\alpha/\nu$ due to $\zeta_\mu^\star=\gamma_C^{2\star}B_{\psi^2}(u_H^\star)=\alpha/\nu$. The time scale of the OP remains at its model A value and is slower than that of the secondary density in agreement with $w_2^\star=0$. In region II $w_2^\star \neq 0$ and the OP and the secondary density 2 are slow with the same time scale. This is expressed by the relation at the fixed point $\zeta_\Gamma^\star=\zeta_\mu^\star=\alpha/\nu$ according to Eq. (58). Thus $z=z_2=2+\alpha/\nu$ and one is in the strong scaling region.

V. NONASYMPTOTIC PROPERTIES OF MODEL $\mathrm{C}^{*\prime}/\mathrm{C}'$

The nonasymptotic behavior is mainly described by the flow of the static and dynamic parameters. The latter are determined by the flow equations (29) with the β functions (28) for the time scale ratios. Because we do not need the static functions at noninteger values of n, as we did in [10] in order to discuss borderlines in the n-d plane, we use now static flow equations with Borel summed ζ functions. This is the reason for differences in the static flow presented in [10] and here.

The static flow equations for u and γ are then (at $d=3$)

$$l\frac{du}{dl}=\beta_u(u), \tag{76}$$

$$l\frac{d\gamma^2}{dl}=\gamma^2(-1+2\zeta_{\psi^2}(u)+\gamma^2B_{\psi^2}(u)), \tag{77}$$

with $B_{\psi^2}(u)=n/2+\mathcal{O}(u^2)$. The Borel-summed functions are

$$\beta_u(u)=-\frac{u}{4!}+4(n+8)\left(\frac{u}{4!}\right)^2\frac{\left(1+a_4\frac{u}{4!}\right)}{\left(1+a_5\frac{u}{4!}\right)}, \tag{78}$$

$$\zeta_{\psi^2}(u)=4(n+2)\frac{u}{4!}\left(1-10\frac{u}{4!}\right)+a_1\left(\frac{u}{4!}\right)^3-a_2\left(\frac{u}{4!}\right)^4. \tag{79}$$

The coefficients a_1,a_2,a_4,a_5 are listed in Table 2 of [16] for integer n values. Using the initial values $u(l_0)/4!=0.000\,25$ and $\gamma^2(l_0)=0.25$ with $l_0=0.1$ we obtain the static flow presented in Figs. 3 and 4 for different n.

While in Fig. 3(a) u reaches its n-dependent fixed point value relatively fast at $l\sim10^{-5}$, the coupling γ in Fig. 4 is much slower. At $n=1$ it reaches the finite value γ_C at $l\sim10^{-10}$ while at $n=2$ it is even at $l=10^{-40}$ considerably different from the fixed value 0. The different fixed points at $n=1$, $n=2$, and $n=3$ are sketched in Fig. 3(b). In the u-γ^2 plane the paths plotted are calculated from the initial values to the fixed points indicated in the figure by different symbols. On the γ^2 axis the unstable fixed point $u^\star=0,\gamma^{\star2}=2/n$ (at $\epsilon=1$) is represented by a square for $n=1$, a circle for $n=2$, and an up triangle for $n=3$. Quite analogously at the u axis the Heisenberg fixed point $u^\star=u_H$, $\gamma^{\star2}=0$, which is stable at $n=2$ and $n=3$, is marked for all three n values. The model C fixed point $u^\star=u_H,\gamma^{\star2}=\gamma_C^2$ is only drawn at $n=1$ (where it is stable). From Fig. 3(b) one can see that the

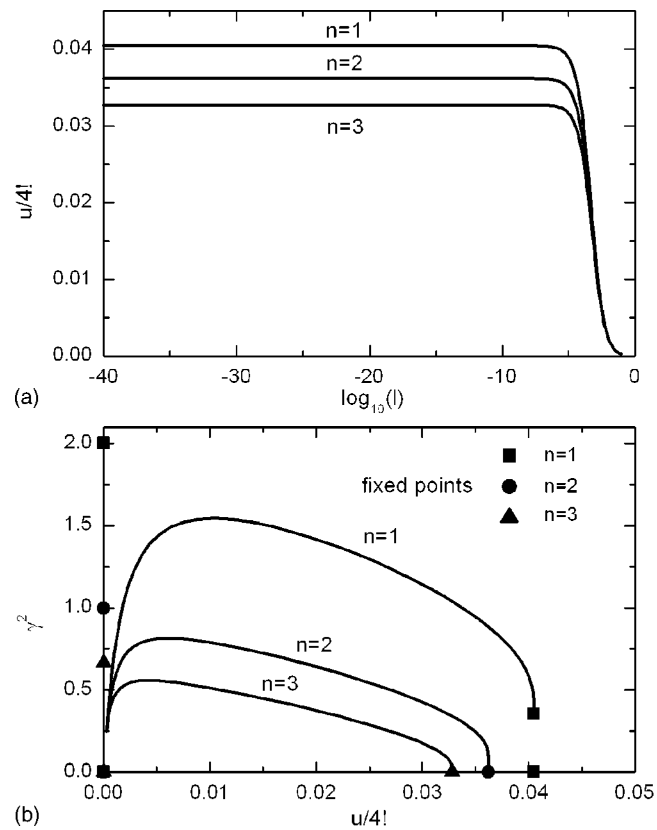

FIG. 3. (a) Flow of the static coupling $u/4!$ at three different order parameter component numbers n. The initial value $u(l_0)/4!$ is in all cases 0.00025. (b) Flow of u [see (a)] and γ^2 (see Fig. 4) in the γ^2- u plane with the inital condition. The fixed points for $n=1,2,3$ are indicated by different symbols.

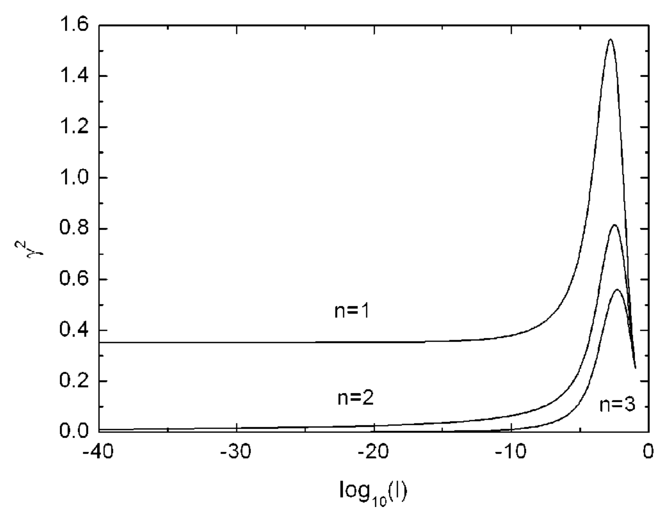

FIG. 4. Flow of the static coupling γ^2 at three different OP component numbers n, corresponding to the u flows in Fig. 3. The initial value is in all cases $\gamma^2(l_0)=0.25$.

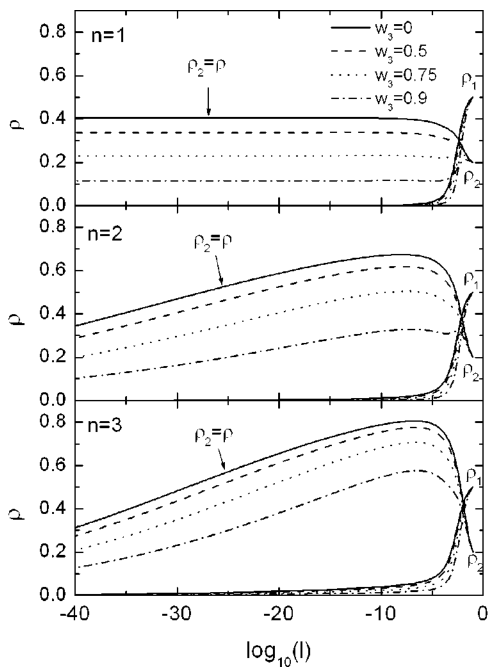

FIG. 5. The flows of ρ_1 and ρ_2 for all three n values at several values of the cross time scale ratio w_3. The flows correspond to the static parameters in Figs. 3 and 4.

values of u and γ^2 are driven first to the unstable fixed point at the γ^2 axis and later change the direction to the stable one. This causes the enhancement in the flow of γ^2 in Fig. 4. Of course this behavior depends on the initial values of u and γ^2 and is obtained at very small $u(l_0)$ and larger $\gamma^2(l_0)$. For small enough $\gamma^2(l_0)$ and/or larger $u(l_0)$ the flow tends directly to the stable fixed point and $\gamma^2(l)$ drops down from starting from the initial value.

The behavior of γ influences the behavior of the flow of the dynamic parameters ρ_i. This is shown in Fig. 5, where we have plotted the flows of ρ_1 and ρ_2 corresponding to the static parameters in Figs. 3 and 4 at several values of w_3 for $n=1,2,3$. ρ_1 drops down to its fixed point value relatively fast. But ρ_2 contains the slow dynamic transient. The transient exponents are listed in Table II from which it is seen that the values of $\omega_\pm$ at $n=1$ are considerably larger than the values at $n=2$ or $n=3$. In the case $w_3=0$ where no coupling between the two secondary densities exists, the flow of ρ_2 is identical to the flow of ρ in model C. From the behavior of the flow we can expect that at $n=2$ and $n=3$ always effective exponents will be observed in experiments or numerical simulations instead of the asymptotic values. Even at $n=1$ where the asymptotics is reached at $l \sim 10^{-10}$ the corresponding exponents will be hardly observable in experiments.

VI. CONCLUSION

We have extended model C to model C′ where two conserved densities couple to a nonconserved OP. It turned out that the asymptotic critical properties of model C′ can be related to those of model C. Although the fixed point value of the ratio of the OP time scale to the time scale of the statically coupled conserved density depends on the Onsager coefficients time scale parameter w_3 [for the definition see Eq. (23)], the dynamical critical exponents and the transient exponents are of course independent of w_3. The nonasymptotic properties however are strongly dependent on this time scale parameter.

As was already shown in model C a fixed point with an infinite ratio of the OP time scale to the conserved density time scale is not stable. Thus one can expect that the problem which appeared at the tricritical point in dynamics mentioned by Siggia and Nelson does not appear in two-loop order [18]. Tricriticality is not described by a fixed point value $w_2^\star=\infty$ as found in the one-loop calculation [5], but by a finite value; this restores scaling for the OP and the corresponding secondary density.

ACKNOWLEDGMENT

This work was supported by the Fonds zur Förderung der wissenschaftlichen Forschung under Project No. 15247–TPH.

APPENDIX A: DIAGONALIZATION OF THE STATIC FUNCTIONAL

In general the structure of the secondary density static functional of model- C*′-type systems is of the form

$$H_q\{\psi_0, q_{i0}\} = \int d^dx \left\{ \frac{1}{2}\boldsymbol{q}_0^T\boldsymbol{A}_q\boldsymbol{q}_0 + \frac{1}{2}\mathring{\boldsymbol{\gamma}}_q^T\boldsymbol{q}_0|\vec{\psi}_0|^2 - \mathring{\boldsymbol{h}}_q^T\boldsymbol{q}_0 \right\}. \tag{A1}$$

The coefficient matrix

$$\boldsymbol{A}_q = \begin{pmatrix} a_{11} & a_{12} \\ a_{12} & a_{22} \end{pmatrix} \tag{A2}$$

is usually related to thermodynamic derivatives in the noncritical background. The matrix elements a_{ij} represent inverse electric or magnetic susceptibilities in the case of electric or magnetic systems, and inverse compressibilities, specific heats, and concentration susceptibilities in the case of fluids, fluid mixtures, or superfluid mixtures (see, for instance, [19–21]). The secondary densities—the couplings to the OP and the external fields—which are chosen to eliminate the finite expectation value of the secondary densities, are written as pseudovectors

$$\boldsymbol{q}_0 = \begin{pmatrix} q_{10} \\ q_{20} \end{pmatrix}, \quad \mathring{\boldsymbol{\gamma}}_q = \begin{pmatrix} \mathring{\gamma}_{q_1} \\ \mathring{\gamma}_{q_2} \end{pmatrix}, \quad \mathring{\boldsymbol{h}}_q = \begin{pmatrix} \mathring{h}_{q_1} \\ \mathring{h}_{q_2} \end{pmatrix}. \tag{A3}$$

The superscript T denotes the transposed quantity. In order to simplify the perturbation expansion a transformation is constructed which diagonalizes the Gaussian part of the secondary densities and eliminates one of the couplings to the OP in one step. Introducing the transformation

$$\boldsymbol{q}_0' = \boldsymbol{M}\boldsymbol{q}_0, \tag{A4}$$

with the transformation matrix

$$\boldsymbol{M} = \begin{pmatrix} 1 & M_{12} \\ M_{12} & M_{22} \end{pmatrix} \tag{A5}$$

and matrix elements

$$M_{12} = \frac{a_{12} - \frac{\gamma_{q_1}}{\gamma_{q_2}} a_{22}}{a_{11} - \frac{\gamma_{q_1}}{\gamma_{q_2}} a_{12}}, \quad M_{21} = \frac{\gamma_{q_1}}{\gamma_{q_2}} M_{22}, \tag{A6}$$

$$M_{22} = \frac{a_{11} - \frac{\gamma_{q_1}}{\gamma_{q_2}} a_{12}}{a_{11} - 2\frac{\gamma_{q_1}}{\gamma_{q_2}} a_{12} + \left(\frac{\gamma_{q_1}}{\gamma_{q_2}}\right)^2 a_{22}}, \tag{A7}$$

one static coupling is eliminated. With Eq. (A4) the static functional (A1) turns into

$$H_{q'}\{\psi_0, q'_{i0}\} = \int d^d x \Big\{ \frac{1}{2} a_1 q'^2_{10} + \frac{1}{2} a_2 q'^2_{20} + \frac{1}{2} \mathring{\gamma}'_2 q'_{20} |\vec{\psi}_0|^2 - \mathring{h}'_2 q'_{20} \Big\}. \tag{A8}$$

Note that the coefficients a_{ij} and the ratio $\gamma_{q_1}/\gamma_{q_2}$ do not renormalize. Therefore the transformation is invariant under renormalization. Rescaling the secondary densities by $m_{i0} = \sqrt{a_i} q'_{i0}$ leads to the expression given in Eq. (11) with corresponding rescaled couplings and external fields. The advantage of transforming the static functional (A1)–(A8) lies not only in the simplified perturbation expansion, but also in a simplified renormalization procedure. In order to conserve the connection between the model- C$^{*}{}'$-type static functional (A1) and the Landau-Ginzburg-Wilson functional (12), which is expressed by relations analogous to Eqs. (14) and (15), under renormalization a matrix formulation of the renormalization procedure is necessary [19]. With a static functional of type (B10) and (11) the usual scalar renormalization scheme can be used.

APPENDIX B: DIAGONALIZATION OF THE DYNAMIC EQUATIONS

The dynamic perturbation expansion gets extremely complex when a nondiagonal kinetic coefficient L, as in Eqs. (3) and (4), is present. In order to perform a two-loop calculation it is absolutely necessary to diagonalize the matrix

$$\mathring{\boldsymbol{\Lambda}}_m = \begin{pmatrix} \mathring{\lambda} & \mathring{L} \\ \mathring{L} & \mathring{\mu} \end{pmatrix} \tag{B1}$$

appearing in the dynamic equations (3) and (4). The eigenvalues of the dynamic coefficient matrix (B1) are

$$\mathring{\lambda}_1 = \frac{1}{2}(\mathring{\lambda} + \mathring{\mu} + \mathring{K}), \quad \mathring{\lambda}_2 = \frac{1}{2}(\mathring{\lambda} + \mathring{\mu} - \mathring{K}), \tag{B2}$$

with

$$\mathring{K} = \sqrt{(\mathring{\lambda} - \mathring{\mu})^2 + 4\mathring{L}^2}. \tag{B3}$$

The diagonal dynamic coefficient matrix is then obtained by

$$\begin{pmatrix} \mathring{\lambda}_1 & 0 \\ 0 & \mathring{\lambda}_2 \end{pmatrix} = \boldsymbol{R}^T \begin{pmatrix} \mathring{\lambda} & \mathring{L} \\ \mathring{L} & \mathring{\mu} \end{pmatrix} \boldsymbol{R}, \tag{B4}$$

where the transformation matrix $\boldsymbol{R}$ is obtained from the eigenvectors corresponding to Eq. (B2). It is an orthogonal matrix ($\boldsymbol{R}^{-1} = \boldsymbol{R}^T$) and has the structure

$$\boldsymbol{R} = \begin{pmatrix} R_{11} & -R_{21} \\ R_{21} & R_{11} \end{pmatrix}, \tag{B5}$$

with

$$R_{11} = \sqrt{\frac{\mathring{\lambda} - \mathring{\mu} + \mathring{K}}{2\mathring{K}}}, \quad R_{21} = \sqrt{\frac{\mathring{\mu} - \mathring{\lambda} + \mathring{K}}{2\mathring{K}}}. \tag{B6}$$

The transformation to a diagonal dynamic coefficient matrix implies the introduction of transformed secondary densities

$$\overline{\boldsymbol{m}}_0 = \boldsymbol{R}^T \boldsymbol{m}_0. \tag{B7}$$

The dynamic equations (3) and (4) reduce to

$$\frac{\partial \overline{m}_{10}}{\partial t} = \mathring{\lambda}_1 \nabla^2 \frac{\delta H}{\delta \overline{m}_{10}} + \theta_{\overline{m}_1}, \tag{B8}$$

$$\frac{\partial \overline{m}_{20}}{\partial t} = \mathring{\lambda}_2 \nabla^2 \frac{\delta H}{\delta \overline{m}_{20}} + \theta_{\overline{m}_2}. \tag{B9}$$

The transformed secondary densities also enter the static functional leading to

$$H_{\overline{m}}\{\psi_0, \overline{m}_{i0}\} = \int d^d x \Big\{ \frac{1}{2} \overline{m}^2_{10} + \frac{1}{2} \overline{m}^2_{20} + \frac{1}{2} \overline{\mathring{\boldsymbol{\gamma}}}^T \overline{\boldsymbol{m}}_0 |\vec{\psi}_0|^2 - \overline{\mathring{\boldsymbol{h}}}^T \overline{\boldsymbol{m}}_0 \Big\}. \tag{B10}$$

The static couplings and external fields transform according to

$$\overline{\mathring{\boldsymbol{\gamma}}} = \begin{pmatrix} \overline{\mathring{\gamma}}_1 \\ \overline{\mathring{\gamma}}_2 \end{pmatrix} = \boldsymbol{R}^T \begin{pmatrix} 0 \\ \mathring{\gamma} \end{pmatrix}, \tag{B11}$$

$$\overline{\mathring{\boldsymbol{h}}} = \begin{pmatrix} \overline{\mathring{h}}_1 \\ \overline{\mathring{h}}_2 \end{pmatrix} = \boldsymbol{R}^T \begin{pmatrix} 0 \\ \mathring{h} \end{pmatrix}. \tag{B12}$$

The perturbation expansion will be performed in the diagonalized dynamic model (1), (2), (B8), and (B9). Introducing time scale ratios

$$\overline{w}_i = \frac{\Gamma}{\lambda_i}, \quad i = 1, 2, \tag{B13}$$

within the dynamically diagonal model, quite analogous to Eq. (23) , we obtain [22]

$$\zeta_\Gamma(u,\{\overline{\gamma}\},\{\overline{w}\}) = \sum_i \frac{\overline{w_i}\overline{\gamma_i^2}}{1+\overline{w_i}}\Bigg\{1-\frac{n+2}{6}u(1-L_A) + \frac{1}{2}\sum_j \frac{\overline{w_j}\overline{\gamma_j^2}}{1+\overline{w_j}}\Bigg(\frac{n+2}{2}L_A - \frac{n}{2} + \frac{\overline{w_i}}{1+\overline{w_i}} + \frac{1}{1+\overline{w_i}}(\overline{w_j^2}l_{ij}^{(a)} - \overline{w_i^2}l_{ji}^{(a)}) + (1+\overline{w_i}-\overline{w_j}) \times \frac{1+\overline{w_i}+\overline{w_j}}{1+\overline{w_i}}l_{ij}^{(s)}\Bigg)\Bigg\} + \zeta_\Gamma^{(A)}(u), \tag{B14}$$

with L_A defined in Eq. (40) for the complex model C$^{*\prime}$ and Eq. (41) for the real model C′. The logarithmic terms are defined as

$$l_{ij}^{(s)} = \ln\frac{(1+\overline{w_i})(1+\overline{w_j})}{1+\overline{w_i}+\overline{w_j}}, \quad l_{ij}^{(a)} = \ln\frac{1+\overline{w_i}}{1+\frac{\overline{w_i}}{\overline{w_j}}}. \tag{B15}$$

The last contribution in Eq. (B14),

$$\zeta_\Gamma^{(A)}(u) = \frac{n+2}{36}u^2\left(L_A - \frac{1}{2}\right), \tag{B16}$$

is the two-loop expression of the corresponding model A function. Neglecting the sum in Eq. (B14) and setting $\overline{w_i} = \overline{w_j} = w$ we obtain the result for model C* presented in [10] [compare Eq. (40) therein]. It is convenient to use the parameters

$$\overline{\rho_i} = \frac{\overline{w_i}}{1+\overline{w_i}}, \quad i=1,2, \tag{B17}$$

which will stay finite when $\overline{w_i}$ tends to ∞ for the real case instead of the time scale ratios. The rewritten ζ function (B14) reads

$$\zeta_\Gamma(u,\{\overline{\gamma}\},\{\overline{\rho}\}) = \sum_i \overline{\rho_i\gamma_i^2}\Bigg\{1-\frac{n+2}{6}u(1-L_A) + \frac{1}{2}\sum_j \overline{\rho_j\gamma_j^2}\Bigg[\frac{n+2}{2}L_A - \frac{n}{2} + \overline{\rho_i} - \frac{\overline{\rho_j^2}(\overline{\rho_j}-\overline{\rho_i})}{(1-\overline{\rho_j})^2}\ln\left(1+\frac{\overline{\rho_i}}{\overline{\rho_j}} - 2\overline{\rho_i}\right) - \frac{(1-2\overline{\rho_j}+\overline{\rho_i\rho_j})(1-\overline{\rho_i\rho_j})}{(1-\overline{\rho_i})(1-\overline{\rho_j})^2}\ln(1-\overline{\rho_i\rho_j})\Bigg]\Bigg\} + \zeta_\Gamma^{(A)}(u). \tag{B18}$$

Inserting the transformation rules [K_ρ is defined in Eq. (35)]

$$\overline{\rho_1} = \frac{2\rho_1\rho_2}{\rho_1+\rho_2+K_\rho}, \quad \overline{\rho_2} = \frac{2\rho_1\rho_2}{\rho_1-\rho_2+K_\rho} \tag{B19}$$

and

$$\overline{\gamma_1} = R_{21}\gamma, \quad \overline{\gamma_2} = R_{11}\gamma, \tag{B20}$$

with matrix elements (B6) rewritten in parameters ρ_i,

$$R_{11} = \sqrt{\frac{\rho_2-\rho_1+K_\rho}{2K_\rho}}, \quad R_{21} = \sqrt{\frac{\rho_1-\rho_2+K_\rho}{2K_\rho}}, \tag{B21}$$

into the above ζ function (B18) we obtain the corresponding expression (33) in the dynamically nondiagonal model.

[1] P. C. Hohenberg and B. I. Halperin, Rev. Mod. Phys. **49**, 435 (1977).
[2] I. E. Dzyaloshinskii and G. E. Volovick, Ann. Phys. (N.Y.) **125**, 67 (1980).
[3] B. I. Halperin, P. C. Hohenberg, and Shang-keng Ma, Phys. Rev. B **10**, 139 (1974) (model C).
[4] R. Folk and G. Moser, Phys. Rev. Lett. **91**, 030601 (2003).
[5] E. D. Siggia, Phys. Rev. B **15**, 2830 (1977); E. D. Siggia and D. R. Nelson, *ibid.* **15**, 1427 (1977).
[6] R. Folk and G. Moser, J. Low Temp. Phys. **136**, 159 (2004).
[7] R. Folk and G. Moser, Phys. Rev. Lett. **89**, 125301 (2002); **93**, 229902(E) (2004).
[8] V. I. Gorentsveig, P. Fratzl, and J. L. Lebowitz, Phys. Rev. B **55**, 2912 (1997).
[9] J. Kockelkoren and H. Chat, Physica D **168-169**, 80 (2002).
[10] R. Folk and G. Moser, Phys. Rev. E **69**, 036101 (2004).
[11] B. I. Halperin, P. C. Hohenberg, and Shang-keng Ma, Phys. Rev. Lett. **29**, 1548 (1972) (model A).
[12] Only in one-loop order does a region $2<n<4$ in the (d, n) plane exist where the fixed point $w^*=\infty$ is stable. This is an artifact of the one-loop approximation.
[13] V. Dohm and R. Folk, Phys. Rev. B **28**, 1332 (1983).
[14] For the case of a real OP relaxation rate the model allows also values $n=1,3,\ldots$ and the results are valid for a n-component OP dynamics.
[15] The values of w_3 are restricted to the interval $]-1,1[$ due to the general condition of positive entropy production.
[16] R. Schloms and V. Dohm, Nucl. Phys. B **328**, 639 (1989).
[17] The difference of $\omega_-^{(l)}$ for $n=1$ to the value in [10] at the end of Sec. IV is due to insertion of the ϵ-expanded fixed point in two-loop order into the one-loop part *and* two-loop part of $\omega_-^{(l)}$.
[18] Due to the structure of the two-loop ζ_Γ function for model F′, the same logarithmic terms appear as in model C′, leading to the instability of a fixed point with a finite value of the static coupling γ and infinite time scale ratio.
[19] G. Moser and R. Folk, Int. J. Low Temp. Phys. **86**, 57 (1992).
[20] G. Moser and R. Folk, Int. J. Low Temp. Phys. **99**, 11 (1995).
[21] R. Folk and G. Moser, Phys. Rev. E **58**, 6246 (1998).
[22] The result for $n=2$ agrees with the corresponding limit of model F′ [7].